

Study of (n,xn γ) reactions on $^{235,238}\text{U}$

A. Bacquias¹, C. Borcea³, Ph. Dessagne¹, M. Kerveno¹, J.C. Drohé², N. Nankov², A.L. Negret³, M. Nyman², A. Plompen², C. Rouki², G. Rudolf¹, M. Stanoiu², J.C. Thiry¹

¹CNRS, Université de Strasbourg, UMR7178, IPHC, 23 rue du Loess, 67037 Strasbourg, France

²EC - Joint Research Center, Institute for Reference Materials and Measurements, Retieseweg 111, B-2440 Geel, Belgium

³Horia Hulubei National Institute of Physics and Nuclear Engineering, Str. Reactorului 30, Bucharest–Magurele, Romania

Abstract

Prompt-gamma spectroscopy and time-of-flight techniques were used to measure (n,xn γ) cross-sections on several nuclei of interest for nuclear reactors. Experiments were performed at the GELINA facility which provides a pulsed white neutron beam of maximum energy about 20 MeV. Preliminary results concerning ^{235}U and ^{238}U will be presented.

1 Introduction

In the context of research and development of future nuclear reactors [1], satisfying to present constraints (environmental impact, security, resources management), studies on fast-neutrons induced reactions play a major role. Indeed, reactions with a threshold, like (n,xn), become important in reactors with a fast spectrum, since they contribute to the neutron multiplication, to the modification of the neutron spectrum and to the production of radioactive nuclei.

There are complementary approaches to measure (n,xn) reaction cross-sections: direct neutron detection, target activation, and prompt γ spectroscopy. Our collaboration chose to rely on that last method. The principle is to use experimental (n,xn γ) cross-sections, and account for unobserved transitions with theoretical predictions, to calculate the total (n,xn) cross-section. In order to reduce this model-dependency, it is primordial to observe a significant part of the total cross-section. In other words, a maximum of transitions has to be treated, especially those going directly to the ground state.

In this context, the aim of the present work is to measure, at high-level precision, the (n,xn γ) cross-sections on ^{235}U and ^{238}U . That latter belongs to the high-priority list of nuclear data [2], for which a significant improvement of accuracy is mentioned.

2 Experimental set-up

The Geel Electron LINear Accelerator (GELINA) located at the Joint Research Center - Institute for Reference Materials and Measurements (Geel, Belgium) provides an intense (compressed) pulsed electron beam. Typical figures for this beam are an energy of 100 MeV, a 1 ns pulse width and a peak-current of 120 A. The maximum repetition rate amounts to 800 Hz; it was used for the experiments mentioned in the present paper. As the electron beam hits the neutron-production target, consisting of Uranium, photons are emitted through the Bremsstrahlung process. Subsequent photonuclear reactions occur, leading to direct and delayed neutrons emission. The produced neutron beam covers a wide energy range, from a few eV to 20 MeV; the maximum of the flux sits between 1 and 2 MeV. The total average flux is about 3.4×10^{13} neutrons per second.

The experimental set-up GRAPhEME is located on Flight Path 16 (FP16), 30 meters away from the neutron-production target. It is represented on fig. 1. The incoming neutron beam passes through a Fission Chamber (FC), consisting of a UF₄ deposit (enriched beyond 99.5% of ^{235}U) embedded in an ionization chamber. The products of neutron-induced fission that escape the deposit leave a signal, whose time and amplitude are stored by the data acquisition system. Knowing the cross-section for $^{235}\text{U}(n,f)$

from evaluations (ENDF/B-VII.0), the fission yields serve as a measure of the neutron flux as a function of the neutron energy.

The neutron energy was obtained using the Time of Flight (ToF) technique. The ToF measurement relied on the start signal T_0 given at the time electrons hit the neutron production target. This reference time is provided by the GELINA facility with a precision of 1 ns.

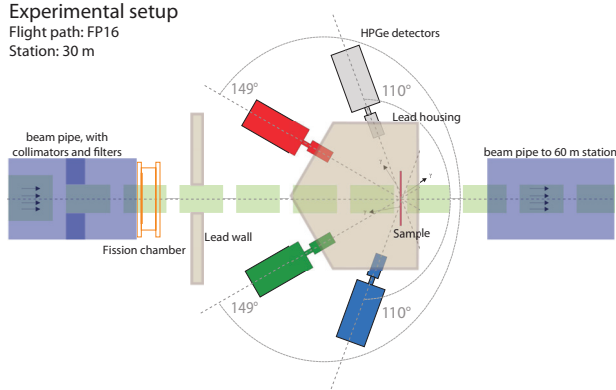


Fig. 1: The GRAPHEME set-up at the GELINA facility on the FP16 - 30m flight-path

In order to perform prompt γ spectroscopy, four planar High-Purity Germanium detectors (HPGe) have been set around a target, consisting of the sample of interest. Neutron-induced inelastic reactions leave the collided nuclei in an excited state. The following de-excitation operates (partly) by gamma-ray emission, detected by the surrounding HPGe.

These HPGe detectors as well as the fission chamber were connected to a fast digital acquisition system using TNT-2 cards working at 100 MHz, developed at IPHC Strasbourg [3]. Events could be recorded with a time precision of 10ns; the energy was coded over 32768 channels.

3 Data analysis

For each HPGe detector, the time distribution of events displays a similar structure as seen in fig. 2. The ambient radioactivity level coming from the set-up itself and surrounding materials adds up with the

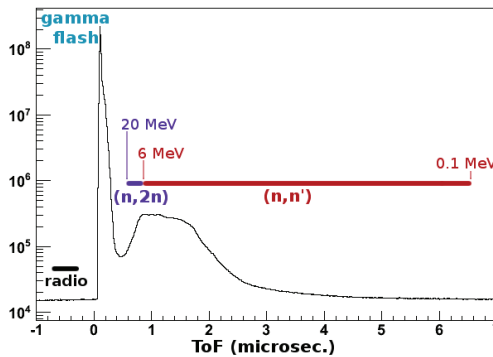


Fig. 2: Part of the ToF distribution, in one HPGe detector.

radioactivity of the sample of interest, forming a constant background, visible on the left on the figure. A

sharp peak occurs as a consequence of the brief emission of gamma rays at the neutron-production target; we refer to it as the “gamma flash”. These events detected in the HPGe detectors are not correlated to neutron-induced reactions. After the gamma flash, gamma events can be linked with incoming neutrons. The first events, corresponding to smallest ToF, are (partially) induced by highest-energy neutrons. With larger ToF come events related to neutrons of less kinetic energy. A time window can be applied to select gamma events as a function of a corresponding neutron energy range. The neutron flux and the precision on the neutron ToF (over a relatively short flight path of 30 metres) put limits on the granularity in neutron energy that we can achieve.

A comparison between a time-gated energy spectrum before and after the gamma flash gives hints of neutron-induced reaction rays. As a function of the location of this gate in the time-distribution, i.e. as a function of the neutrons mean energy, peaks rise and disappear. This phenomenon is visible in two-dimensional histograms such as fig.3, where a part of the energy distribution is displayed as a function of a part of the ToF distribution. The gamma flash is seen as a strong vertical line. Horizontal lines starting from the left, so before neutrons arrive, correspond to radioactivity rays. On the right hand side of the gamma flash, i.e. when neutrons arrive, some rays appear, and slowly fade away.

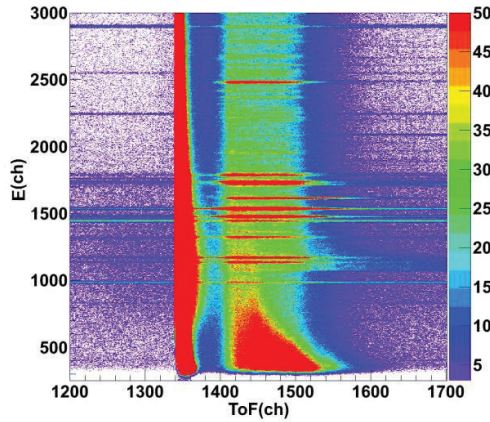


Fig. 3: Partial energy distribution vs partial ToF distribution (in channels), in one HPGe detector.

Once “spotted”, a reaction ray is followed throughout the whole acquisition time gate. A collection of time intervals is prepared, for which we determine the corresponding neutron energy ranges. For each of these intervals, we determine the number of counts contained within the peak of interest. This procedure applies to each of our HPGe.

The formula expressing the reaction cross-section for one gamma transition as a function of our observables is as follows:

$$\sigma = \frac{N_\gamma}{\epsilon_\gamma} \frac{\epsilon_{\text{FC}}}{N_{\text{FC}}} \sigma_{235\text{U}}(n, f) \frac{N_{235\text{U}}}{N_{\text{sample}}}, \quad (1)$$

with N_γ the number of detected gamma events, ϵ_γ the detector’s efficiency for that γ energy, N_{FC} the number of detected fission products in the Fission Chamber (FC), ϵ_{FC} the FC efficiency, N_{sample} the number of atoms in the sample and $N_{235\text{U}}$, the number of ^{235}U atoms in the FC deposit.

In the frame of high-precision studies, specific efforts were put on the quantification of the uncertainties. Besides the obvious need for large statistics with background reduction, careful simulations and calibrated-source measurements have been performed to determine detectors efficiencies. In addition, the Uranium deposit inside the FC and the target sample were precisely characterized (dimensions, mass, purity).

The integration of the differential cross-sections over all angles is performed using the Gauss quadrature. The method applied to γ -ray yields is explained in ref. [4]. In the present experiment, the measurement of the differential cross-section of a given transition at two appropriately chosen angles is sufficient to calculate the angle-integrated reaction cross-section:

$$\sigma = 4\pi \left[w_1 \frac{d\sigma}{d\Omega}(\theta_1) + w_2 \frac{d\sigma}{d\Omega}(\theta_2) \right], \quad (2)$$

where angles $\theta_1 \approx (30.6^\circ \text{ or } 149.4^\circ)$ and $\theta_2 \approx (70.1^\circ \text{ or } 109.9^\circ)$ are roots of the Legendre polynomial $P_4(\cos\theta)$, with associated coefficients $w_1 \approx 0.35$ and $w_2 \approx 0.65$.

4 Experimental results

We will present here the results concerning $(n,n'\gamma)$ and $(n,2n\gamma)$ reaction cross-sections for ^{235}U and ^{238}U . The characteristics of each sample used as a target are summed up in table 1.

Table 1: Specifications of the ^{235}U and ^{238}U targets

Isotope	Enrichment (%)	Total mass (g)	Diameter (cm)	Thickness (mm)
^{235}U	93.20(3)	37.43(1)	12.004(4)	0.211(6)
^{238}U	99.9(?) ^a	10.61911(7)	7.019(9)	0.18(4) ^a

^a As given by the manufacturer; all other quantities were measured with high precision at IRMM.

4.1 The case of ^{235}U

The analysis and results of the $(n,2n\gamma)$ reactions on ^{235}U will be discussed in more details in a forthcoming article [5]. Data were accumulated over more than 1400 hours of beam time. Angle-integrated cross-sections of one $(n,n'\gamma)$ and three $(n,2n\gamma)$ reactions have been obtained with a precision about 5-7 % below 9 MeV, degrading to about 20 % for higher energies (mainly due to low neutron flux).

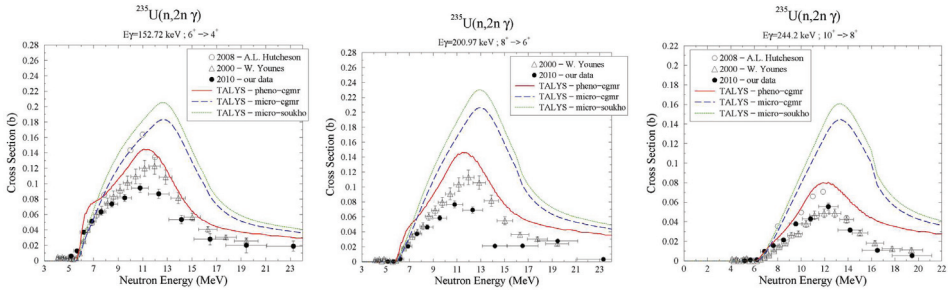


Fig. 4: Cross-sections of $(n,2n\gamma)$ reactions on ^{235}U as a function of incident neutron energy.

The $(n,2n\gamma)$ cross-sections for three γ transitions are plotted in fig. 4 as a function of incident neutron energy. Our data are compared to experimental results of Younes et al. [6] and Hutcherson et al. [7] when available. TALYS predictions are also displayed for three different calculations, using different input models. Data sets agree between themselves on the shape of these cross-sections. The shape is also well reproduced by the phenomenological approach with TALYS. The other two TALYS calculations yield substantial overestimation of the cross-sections, compared to data. Quantitative discrepancies between data sets remain.

4.2 The case of ^{238}U

Data were accumulated over more than 1200 hours of beam time. Angle-integrated cross-sections of $(n, xn\gamma)$ for about 20 γ have been extracted, including three $(n, 2n\gamma)$ and four $(n, 3n\gamma)$ that are not shown here. The ^{238}U results are preliminary, especially in the sense that the determination of systematic uncertainties is still under process. The figure displayed below accounts only for statistical uncertainties.

We could extract several cross-sections for transitions in the main band, and many more from other rotational bands. A few transitions going to the ground state were analyzed, including the deexcitation of the first level at 45 keV (very preliminary results, with arbitrary error bars).

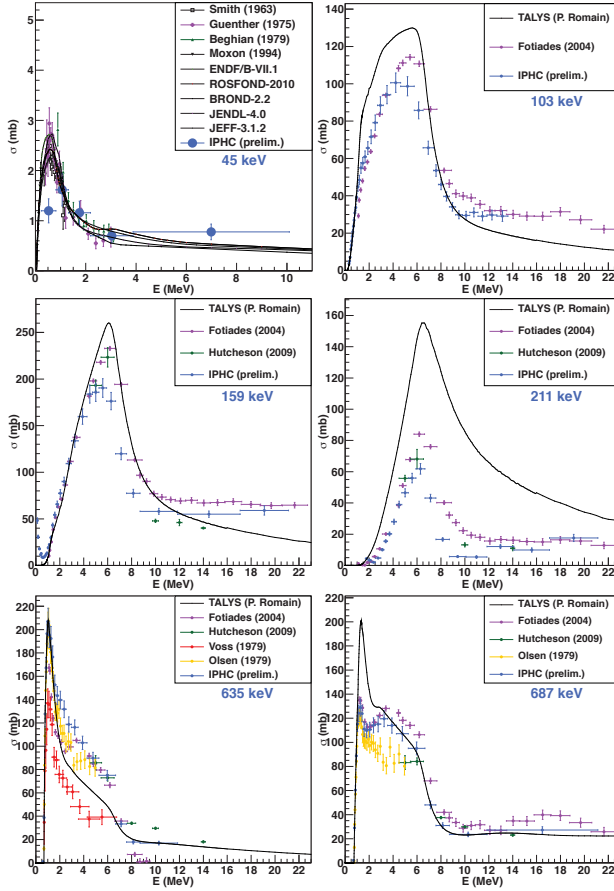


Fig. 5: Cross-sections of $(n, n'\gamma)$ reactions on ^{238}U as a function of incident neutron energy.

Six transitions are presented in fig. 5: the four lowest transitions in the main band, 44.9 keV ($2^+ \rightarrow 0^+$), 103.5 keV ($4^+ \rightarrow 2^+$), 159.3 keV ($6^+ \rightarrow 4^+$), 211 keV ($8^+ \rightarrow 6^+$), and two transitions from second-band levels, 635 keV ($1^- \rightarrow 2^+$) and 687 keV ($3^- \rightarrow 2^+$). Our data are compared to experimental results from Voss [8], Olsen [9], Fotiades [10], Hutcheson [11] and their collaborators. Calculations performed by P. Romain [12] with TALYS are presented, except for the first level, where the disagreement goes out of scale. The cross-section for the first level (45 keV) is compared to direct neutrons measurements by Smith [13], Guenther [14], Beghian [15], Moxon [16] and their collaborators, and a list of evaluations: ENDF/B-VII.1, ROSFOND-2010, BROND-2.2, JENDL-4.0, and JEFF-3.1.2.

No strong tendency can be noticed from fig. 5. TALYS calculations are generally in good agreement with data regarding the shape of the cross-section, with the notable exception of the 687 keV (and a few other transitions, not shown here). Concerning the magnitude of these predictions, they are much too high for the 45 and the 211 keV. One of the limitations of these calculations is that despite the inclusion of thirty discrete levels, a few important levels decaying directly towards the ground state (e.g. 1279 keV) are not described. Data agree rather well between themselves. The compatibility between our data and direct neutron measurements of the first level production is encouraging.

5 Conclusion

For the two actinides ^{235}U and ^{238}U , the development of a dedicated set-up and analysis techniques allowed to perform experiments relying on prompt gamma spectroscopy and time of flight measurements. We could extract angle-integrated reaction cross-sections for $(n,xn\gamma)$ processes with a typical precision ranging from 5 to 7 % below 9 MeV, and to about 20 % for higher energies. The authors bear in mind the importance of an exhaustive review of systematic uncertainties and of the determination of the covariance matrix.

The extremely sensible measurement of first levels' deexcitation is guiding further evolutions of the current GRAPhEME set-up. The minimization of the attenuation for low-energy gamma rays will be a first step, before considering the measurement of internally converted electrons.

Extensions of our experimental equipment will occur with two additional planar HPGe, that will be followed later by a 36-pixels planar HPGe. Measurements of $(n,xn\gamma)$ reactions on very active targets like ^{233}U are foreseen in the near future.

Acknowledgements

The authors wish to thank the team of the GELINA facility for the preparation of the neutron beam and for their strong support day after day. This work was supported by the European Commission within the Sixth Framework Programme through I3-EFNUDAT (EURATOM contract no. 036434) and NUDAME (Contract FP6-516487), and within the Seventh Framework Programme through EUFRAT (EURATOM contract no. FP7-211499) and through ANDES (EURATOM contract no. FP7-249671).

References

- [1] The Generation IV International Forum, <http://www.gen-4.org/>.
- [2] OCDE-NEA, Nuclear Data High Priority List, <http://www.oecd-nea.org/dbdata/hpr1/>.
- [3] Electronics group for nucl. phys. at IPHC Strasbourg, <http://www.iphc.cnrs.fr/-tnt-.html>.
- [4] C.R. Brune, Nucl. Instr. Meth. Phys. A 493 (2002) 106-110.
- [5] J.-C. Thiry et al., $^{235}\text{U}(n,n'\gamma)$ and $^{235}\text{U}(n,2n\gamma)$ reaction cross sections, to be submitted (2012).
- [6] W. Younes et al., Tech. Rep. UCRL-ID-140313, U.S. Dept. of Energy, LLNL (2000).
- [7] A.L. Hutcheson, Ph.D. thesis, Dept. of Physics in the Graduate School of Duke University (2008).
- [8] F. Voss, Kernforschungszentrum Karlsruhe Reports, No.2379 (1976).
- [9] D.K. Olsen, Conf.on Nucl.Cross Sections F.Techn.,Knoxville 1979, p.677.
- [10] N. Fotiades et al., Phys. Rev. C 69, 024601 (2004).
- [11] A.L. Hutcheson et al., Phys. Rev. C 80, 014603 (2009).
- [12] Private communication.
- [13] A.B. Smith et al., Nucl. Phys. 47 (1963), p.633.
- [14] P. Guenther et al., Argonne National Laboratory Reports 16 (1975).
- [15] L.E. Beghian et al., Nuclear Science and Engineering 69 (1979), p. 191.
- [16] M.C. Moxon et al., Conf.on Nucl.Data for Sci.and Techn., Gatlinburg 1994, p.981.